Acta Cryst. (1971). A27, 586

Direct Analysis of Small-Angle Equatorial X-ray Scattering from Fibrous Systems. I. Expressions for the Intensity and Patterson Function

BY P. J. HARGET* AND S. KRIMM

Biophysics Research Division and Department of Physics, University of Michigan, Ann Arbor, Michigan, U.S.A.

(*Received* 30 *November* 1970)

Small-angle equatorial X-ray scattering from fibrous systems is often complicated by the effects of morphological organization and/or heterogeneities, as well as by macromolecular structure and organization influencing this same region of scattering space. The problem is not easy to solve. As a new approach, a technique has been developed that entails a direct quantitative analysis of the Patterson function. It is shown that when the intensity data are purposely truncated at appropriate points, the Patterson function can be expressed as a closed-form mathematical function of the truncation points and parameters describing the scattering system. This allows a direct analysis of the Patterson function and an accurate extraction of the parameters describing the scattering system without prior knowledge of these parameters.

1. Introduction

Most of the methods developed for normal high-angle X-ray analysis could, in principle, be applied to small-angle X-ray scattering. Unfortunately, structural inhomogeneities and lattice distortions yield a diffraction pattern that is extremely difficult to analyze. The effects of both factors are seen in the high-angle region, but because of the rather large size of the structural inhomogeneities they give rise to, or dominate, the small-angle region of the diffraction pattern on the equator. This small-angle scattering has been observed in many natural fibrous systems: keratins (Corey & Wyckoff, 1936, Krimm, 1963), silk fibroin and lobster chitin (Corey & Wyckoff, 1936), cellulose (Corey & Wyckoff, 1936, Heikens, Hermans & Weidinger, 1952, Heyn, 1948), bone (Engstrom & Finean, 1953), bacterial flagella (Astbury & Weibull, 1949), F-actin (Astbury & Sparks, 1947, Astbury, 1949), and collagen (North, Cowan & Randall, 1954).

Many models have been proposed to explain some of the small-angle scattering, *e.g.* a limited hexagonal lattice (Burge, 1963), a cylindrical lattice (Sasisekharan & Ramachandran, 1957), layered arc lattices (Krimm, 1967), and multiple aggregates (Burge, 1961); but there have been relatively few attempts to analyze directly small-angle diffraction data. Bear & Bolduan (1950) devised a scheme whereby the size of the micelles or crystallites can be estimated directly from the diffraction pattern; however, due to other structural effects their scheme has not been too useful. Perhaps one of the best attempts to date was that of Hosemann (1967) in the direct semiquantitative analysis of linear polyethylene, where both the small- and high-angle diffractions in the framework of polydispersity and paracrystallinity were considered.

The problem was approached more directly by the use of a radial-distribution function analysis (Heyn, 1955). This technique, however, suffers from the fact that the fibrillar scattering factor must be known; since this is not true in most cases, it must be assumed. The use of a radial-distribution function analysis also imposes the conditions of an isotropic, homogeneous scattering system that is infinite in extent (James, 1948), conditions usually not satisfied in a fibrous system.

In an attempt to explain the small-angle equatorial X-ray scattering of several fibrous biological systems quantitatively, and to avoid assumptions about the scattering system, we have developed a technique for the direct analysis of these data involving a direct quantitative analysis of the Patterson function.

2. Forced truncation and expressions for equatorial intensity

The analysis of any X-ray diffraction pattern begins with an expression for the intensity, which is a function of the various parameters describing the scattering system. Since this work depends on such an expression, a brief review at this point is not only helpful but necessary to define appropriate points to truncate the equatorial intensity. Also, the expressions are rewritten to yield a more meaningful interpretation and are modified to account for non-ideal factors, *i.e.*, distortion effects, structural inhomogeneities, and finite crystallite size.

An expression for the intensity of scattering from a non-ideal fibrous system that is valid for the whole of scattering space would be very complex. However, if only equatorial intensity is used in an analysis, then the synthesized fibril is infinite in extent along its

* Present address: Allied Chemical Corporation, Corporate Chemical Research Laboratory, Morristown, New Jersey 07960, U.S.A.

fiber axis (z axis), and the synthesized electron density of the fibril is the projection of the fibril onto the $x-y$ plane. Further, if the fibrils are roughly circular in cross section and, for example, twist or wind along their length, then the projected electron density is close to being cylindrically symmetric. Also, no matter what disposition the fibrils have with respect to their c-axis synchronization, the interfibrillar interference due to lateral organization is undisturbed on the equator (James, 1948).

Although the mathematical form of the functions for the Fourier transform of the fibril and interfibrillar interference are simplified by the restriction of an equatorial intensity analysis, the actual functions are still unknown and are not segregated. Also, distortion effects and structural inhomogeneities in the intensity remain complex.

If the equatorial intensity is restricted by using only intensity out to, and including, the first-order reflection on the equator, then the following implications and simplifications result:

(a) The paracrystalline distortion parameter (Δ) can be neglected as a first approximation, if Δ/S_1 (S_1 is the average first nearest-neighbor distance between fibrils in a plane perpendicular to the fiber axis) is less than about 5%, *i.e.* the first few reflections are undistorted or crystalline (Hosemann & Bagchi, 1962). This fact is not used in the derivations and, hence, does not restrict our results; however, since many fibrous systems do satisfy this condition, it is discussed in the next section.

(b) The effect of truncating the intensity just outside the first-order reflection at k_0 allows information of only a smeared fibrillar structure to be obtained. To express this more quantitatively, we define $k=4\pi \sin\theta/\lambda$, where λ is X-ray wavelength and 2θ is the scattering angle, and let:

$$k_0 \equiv 4\pi \sin\theta_0/\lambda \simeq 2\pi/S_1, \qquad (1)$$

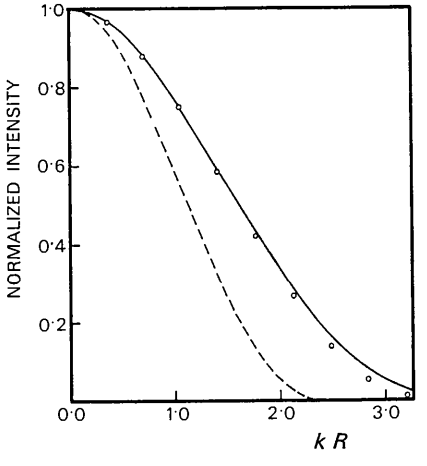

Fig. 1. Small-angle intensities for a solid cylinder (—I_{SC}), a thin shell cylinder (– – –I_{TS}), and the affine transformation (○ ○I') which shows their equivalence.

where S_1 is the first nearest-neighbor separation. From (1) we see that if $S_1 \simeq$ diameter of the fibrils, the smallest structure that can be resolved is the order of 0·6 times the diameter of the fibrils (James, 1948).

(c) Because structural inhomogeneities are on a scale larger than the fibrils, they can be resolved. However, they are not easily interpreted. Their influence on the intensity in the small-angle region may broaden the 000 reflection, as well as other peaks, and may induce subsidiary non-Bragg maxima.

(d) Any amorphous or matrix material can be considered as a constant electron density. This implies that the matrix structure is either small compared to the size of the fibrils, as in many biological systems, or it is disorganized to the point where it yields only high-angle scattering.

(e) The smearing out of the structure of the fibril allows the fibril in this low-angle region to be treated as a continuous electron density. Combining this with the consequences of an equatorial analysis insures that the fibril can be described by a continuous radial electron density, *i.e.*, the electron density is cylindrically symmetric; thus, $\overline{|F|^2}=|\bar{F}|^2=FF^*$, where F is the Fourier transform of the fibril.

(f) In this low-angle region the intensity of a single fibril, FF^*, can be expressed in terms of a single parameter as $4J_1^2(kR_e)/(kR_e)^2$, where R_e is an equivalent radius. This can be seen by considering the scattering from cylindrically symmetric rods with different radial electron densities. According to Oster & Riley (1952), normalized intensities for a solid cylinder and an infinitesimally thin cylindrical shell, both of radius R, are respectively:

$$I_{SC}=4J_1^2(kR)/(kR)^2$$
$$I_{TS}=J_0^2(kR)\,.$$

These are shown as a function of kR in Fig. 1. By a simple affine transformation of the thin-shell intensity, $I'=J_0^2(kR/\sqrt{2})$, Fig. 1 shows that this new function has a shape almost identical to that of I_{SC} in the region $kR\leq 3$, even though electron densities are greatly different. Also, calculations with Gaussian distributions, step functions, and other radial electron densities all show the same type of result. (This merely exemplifies the implications given in (b) of this section.) From equation (1), $k_0R_e\leq\pi$ since $S_1=2R_e$ is a minimum value for S_1. Hence, the intensity of a single fibril in this region is

$$FF^*=4J_1^2(kR_e)/(kR_e)^2, \qquad (2)$$

where R_e is the radius of an equivalent solid cylinder.†

(g) Although R_e is used in calculations, it can be interpreted in terms of a radius of gyration. In the very small-angle region, $kR\ll 1$, the intensity of a rod-shaped particle can be expressed by a generalized Guinier approximation (Guinier & Fournet, 1955) as

† In actual calculations it was found that $k_0R\leq 2{\cdot}5$ was sufficient to include the first-order reflection.

$$I_G = \exp[-k^2 R_G^2/2],$$

where R_G is the radius of gyration with respect to the electron density.

By expanding in a Taylor series about the origin:

$$I_G \simeq 1 - \frac{k^2 R_G^2}{2} + \ldots .$$

Since

$$I = 4\frac{J_1^2(kR_e)}{(kR_e)^2} \simeq 1 - \frac{k^2 R_e^2}{4} + \ldots ,$$

then

$$R_G = R_e/\sqrt{2} . \tag{3}$$

Next, consider a paracrystallite† composed of N parallel fibrils, where the fiber axis is in the z direction. To avoid any assumption about the size of the paracrystallite, N is considered a parameter. The equatorial intensity of the paracrystallite is

$$I(\mathbf{k}) = \sum_{i=1}^{N}\sum_{j=1}^{N} F_i^* F_j \exp[i\mathbf{k} \cdot (\mathbf{r}_i - \mathbf{r}_j)] ,$$

where: F_i is the Fourier transform of the ith fibril, and $\mathbf{r}_i$ defines the position of the ith fibril in real space which is confined to the $x-y$ plane.

Using equation (2):

$$I(\mathbf{k}) = C\frac{J_1^2(kR_e)}{(kR_e)^2}\sum_{i=1}^{N}\sum_{j=1}^{N}\exp[i\mathbf{k} \cdot (\mathbf{r}_i - \mathbf{r}_j)] ,$$

where C is a constant containing atomic numbers, *etc.*

If there are many such groups of N fibrils, where each group is the same geometrically but the groups are randomly oriented with respect to one another about their own centroidal z axes and scattering independently, then according to Oster & Riley (1952):

$$I(k) = C\frac{J_1^2(kR_e)}{(kR_e)^2}\sum_{i=1}^{N}\sum_{j=1}^{N} J_0(kr_{ij}) ,$$

where $J_0(kr_{ij})$ is a zero-order Bessel function and $r_{ij} = |\mathbf{r}_i - \mathbf{r}_j|$.

Normalizing, so that $I(O) = 1$:

$$I(k) = \frac{4J_1^2(kR_e)}{(kR_e)^2}\frac{1}{N^2}\sum_{i=1}^{N}\sum_{j=1}^{N} J_0(kr_{ij}) .$$

Since r_{ij} is only a scalar quantity, a considerable simplification results by grouping the r_{ij}'s of the same length and designating this length by a single index i; then the intensity can be rewritten as:

$$I(k) = \frac{4J_1^2(kR_e)}{(kR_e)^2}\frac{1}{N^2}\sum_{i=0}^{m} A_i J_0(kS_i) \tag{4}$$

where:

m is the number of *different* interfibrillar vector lengths in a paracrystallite,

S_i is the ith vector length, *e.g.* S_1 is the first nearest-neighbor separation in real space,

A_i is the number of fibrils separated from any other fibril by the vector length S_i; hence, A_i is also the number of fibrils at a given vector length S_i in a Patterson function.

Note also that $S_0 = 0$, $A_0 = N$, $I(O) = 1$.

In real systems the number of fibrils, N, in any coherent group or paracrystallite is not a constant, *i.e.* N varies between groups. However, this is easily taken into account by usual averaging procedures, and the resulting expression for the normalized intensity is:

$$I(k) = \frac{4J_1^2(kR_e)}{(kR_e)^2}\frac{1}{\langle N^2\rangle}\sum_{i=0}^{\bar{m}}\langle A_i\rangle J_0(kS_i) . \tag{5}$$

This equation is identical to equation (4), except that parameters A_i and N^2 must now be considered as average values and $\bar{m}$ is now the maximum number of different vector lengths present in the largest paracrystallites.

So far the lattice has been treated as if it were discrete (single values of S_i). However, two-dimensional lattice distortions are present in any real system, and to keep the approach general they must be accounted for. To incorporate lattice distortions in an expression for the intensity, let $W_i(S)$ be a distribution function describing the distortions about the ith difference vector length S_i, normalized so that

$$\int W_i(S)\mathrm{d}V_s = 1 .$$

It is easily shown that the expression for the normalized intensity becomes:

$$I(k) = \frac{4J_1^2(kR_e)}{(kR_e)^2}\frac{1}{\langle N^2\rangle}\sum_{i=0}^{\bar{m}}\langle A_i\rangle \times \int W_i(S)J_0[k|\mathbf{S}_i + \mathbf{S}|]\mathrm{d}V_s , \tag{6}$$

or

$$I(k) = \frac{4J_1^2(kR_e)}{(kR_e)^2}\frac{1}{\langle N^2\rangle}\sum_{i=0}^{\bar{m}}\langle A_i\rangle J_0(kS_i) \times \int W_i(S)J_0(kS)S\mathrm{d}S . \tag{7}$$

These two equations are equivalent, differing only in the order of integration; however, the first is the most logical to visualize, whereas the second is the easiest to use.

Note that these equations are also valid for $k > k_0$, when F is used for the scattering factor, but k must be small enough so that the matrix can still be treated as a constant and $\overline{F^2} = \bar{F}^2$ is still valid. Two examples for specific $W_i(S)$'s are as follows:

Case (*a*): $W_i(S) = \delta(\mathbf{S})$, *i.e.*, a delta function in $\mathbf{S}$. Then:

$$\int \delta(\mathbf{S})J_0[k|\mathbf{S}_i + \mathbf{S}|]dV_s = J_0(kS_i) .$$

† A paracrystal is used since it is very general and can describe many types of lattices.

Hence:

$$I=\frac{F^2}{\langle N^2\rangle}\sum_{i=0}^{\bar{m}}\langle A_i\rangle J_0(kS_i)\,.$$

Case (*b*): $W_i(S)=(1/\sigma_i^2)\exp[-S^2/2\sigma_i^2]$, *i.e.*, a Gaussian distribution.
Then:

$$1/\sigma_i^2\int_0^\infty \exp[-S^2/2\sigma_i^2]SJ_0(kS)dS=\exp[-k^2\sigma_i^2/2]\,.$$

Hence:

$$I=\frac{F^2}{\langle N^2\rangle}\sum_{i=0}^{\bar{m}}\langle A_i\rangle \exp[-k^2\sigma_i^2/2]J_0(kS_i)\,. \qquad (8)$$

As a final consideration for expressing the equatorial intensity, allowances must be made for structural inhomogeneities although they would be almost impossible to incorporate even if they were known and could be parametrized. However, one of the main effects of structural inhomogeneities is to cancel interference between paracrystallites or bundles; then the scattering can be described as that due to an average bundle (it is in this sense that the term limited coherency is used). Examples are the well-known Scherrer line broadening formula or polydispersity of micellar and fibrillar systems as given by Hosemann & Bagchi (1962).

This effect is introduced in two ways: by geometric inhomogeneities and by electron-density fluctuations. If the structural inhomogeneities are geometric in nature, such as: nematic or smectic stacking of the bundles, fibrillarity of the bundles, regions of parallelism and non-parallelism, polydispersed bundle sizes, or simply a curvilinear lattice causing limited bundle size, then equation (7) adequately represents the intensity by leaving $\bar{m}$, which accounts for the average coherent size, as a free parameter.

If, however, an electron-density fluctuation associates with the coherent bundle (*e.g.*, that brought about by chain-folding in some synthetic polymers), then a problem arises. There is an additional contribution to the 000* reflection due to the fluctuation (Harget, 1969). There are three cases to consider:

(1) If the electron-density fluctuation is small (*e.g.*, that caused by preferential bonding between fibrils which set up the geometric structural inhomogeneities) and is small relative to the electron-density difference between fibrils and the matrix, then equation (7) is adequate to describe the system no matter what the average bundle size is.

(2) If the average bundle size is very large, then the 000 reflection is unobservable, and again equation (7) is adequate to describe the system.

(3) If electron-density fluctuations are not negligible, and if average bundle size is small, then the contribution to the 000 reflection cannot be neglected.

At first glance, this last case seems to complicate matters to the point where the structure can not be solved because the electron-density fluctuations are not known. However, in actual experiments only the outer portion of the 000 reflection can be obtained; thus, equation (7) can be used again as a fair approximation whose effect will only cause, at worst, an underestimation of bundle size. A check on the validity of this approximation is the consistency of the average bundle size obtained with other features of the small-angle scattering pattern, such as integral width of the first-order equatorial reflection, or the breadth of low-order meridional reflections perpendicular to the fiber axis.

Although equation (7) adequately describes the small-angle equatorial intensity, its use has practical limitations. If the paracrystallites or bundles are moderately small in size, then equation (7) is practical to use. On the other hand, if the size of paracrystallites is large, equation (7) is impractical to use because of the large number of fibrils, N, in an average crystallite and a correspondingly large number of interfibrillar vector lengths, S_i. Also, as the index i increases, vector lengths become closer to each other (*e.g.* in a crystal, $|d_{hkl+1}/d_{hkl}|$ decreases towards unity as the indices increase). This, combined with the fact that paracrystalline distortions increase with the index i, results in a continuum of S_i's for large values of the index i.

By letting the interfibrillar vector lengths be described by a distribution function $G(S)$, and assuming the sizes of the paracrystallites to be so large that the region where $G(S)$ fluctuates is much smaller than the largest vector length present in an average paracrystallite, then, according to Oster & Riley (1952):

$$I(k)=F^2\{1-v\int_0^\infty 2\pi S[1-G(S)]J_0(kS)\mathrm{d}S\}\,, \qquad (9)$$

where F is the scattering factor of a single fibril and v is the density of fibril centers in a lateral plane; also, $I(O)=1$. Equation (9) is analogous to equation (7) and is valid *only* for very large bundles or paracrystallites. Also, equation (9) has the advantage over equation (7) in that counting of the vector lengths is avoided, and the paracrystalline lattice distortions are already in $G(S)$. However, a serious practical difficulty arises if equation (9) is inverted *via* a radial distribution function analysis. This is discussed in the next section.

3. Patterson function versus a radial distribution function analysis

When solving a scattering problem, a direct approach is possible through the Patterson function. However, the Patterson function is in general very difficult to interpret. On the other hand, a semidirect inversion of the intensity data through a radial distribution function analysis provides a means of making the inter-

* The term 000 reflection represents the rise into the origin of reciprocal space along the equator. Note that if the superlattice (lattice formed by the paracrystallites) is reasonably ordered, there may be at least a first-order peak in this 000 reflection. However, that possibly is ignored in this paper so as not to obscure the method of approach. If such a case exists, the theory can be modified easily to handle it.

pretation quite simple, though it has a serious practical difficulty: F, the scattering factor of a single fibril, must be known before performing the inversion process.

If the intensity is purposely truncated at k_0, then F is given by equation (2), but a serious truncation error results from the inversion process, even when the correct R_e is known. Recall that the first few peaks in $G(S)$ for a paracrystal have half-widths of approximately 2Δ, 4Δ, *etc.* In a fibrous system (*e.g.*, the keratins), Δ/S_1 is of the order of 5 or 6% (Hosemann, 1951). If the intensity is multiplied by a step function of width k_0, $G(S)$ is convoluted with the transform of this step function. As a result, any peaks in $G(S)$ are broadened to a minimum half-width of the order of 0·6 S_1, hence obscuring small paracrystalline distortions. For a liquid this is not too serious a problem, since even the first peak in $G(S)$ is very broad. But for a paracrystal with relatively small Δ/S_1 the function, $G(S)$, obtained by truncating at k_0 and inverting, is not very meaningful because of the mentioned broadening, and such aspects as nearest-neighbor numbers would be very inaccurate.

A further well-known problem is to determine the correct scaling factor for F^2 when I/F^2-1 is formed before the inversion. Finally, a complication arises from the fact that R_e is usually an unknown to be determined after the inversion. The whole truncation problem could be avoided by extending k_0 to include higher orders in the diffraction data, but then F would again be an unknown. In conclusion, a radial-distribution function analysis of fibrous systems, even if the paracrystallites were large, would not be very fruitful.

The alternative is to use a Patterson function. Since the Patterson function is simply the Fourier transform of the intensity, it is not necessary to know F for the inversion; also, in the vicinity of the Patterson origin, the convolution of the fibril with itself is present, which can give information about the fibril alone. In addition, the fibril, convoluted with itself, is located at each nearest-neighbor peak; thus, the half-widths of all the peaks without the truncation error due to k_0 would have a minimum value of the diameter of the fibril, or approximately S_1. Consequently, convoluting with a function of half-width 0·6S_1 would not have as severe effects as it has in a radial distribution function analysis. The only problem that remains is to obtain a mathematical formulation of the Patterson function in terms of the general expressions for the intensity, and to examine the quantitative effect of k_0.

4. Patterson functions – resolution and formulation for cylindrically symmetric equatorial scattering

In general, the Patterson function is defined as:

$$P(\mathbf{r}) \equiv \iiint_{-\infty}^{\infty} \varrho(\mathbf{r}')\varrho(\mathbf{r}'-\mathbf{r})\mathrm{d}V_{r'} ,$$

where $\varrho(\mathbf{r})$ is the electron density of the scattering system.

The Patterson function, $P(\mathbf{r})$, is also the Fourier transform of the intensity; thus, for the $x-y$ plane:

$$P(x,y) = \frac{1}{(2\pi)^2} \iint_{-\infty}^{\infty} I(k_x,k_y) \times \exp\left[-i(k_x x + k_y y)\right]\mathrm{d}k_x\mathrm{d}k_y ,$$

or in cylindrical coordinates:

$$P(r,\varphi) = \frac{1}{(2\pi)^2} \int_0^{\infty} k\mathrm{d}k \int_0^{2\pi} I(k,\varphi_k) \exp\left[-i\mathbf{k}\,.\,\mathbf{r}\right]\mathrm{d}\varphi_k .$$

Imposing the restriction that $I(k,\varphi_k)$ is a function of k only, and integrating over φ_k, yields:

$$P(r) = \frac{1}{2\pi} \int_0^{\infty} I(k)J_0(kr)k\mathrm{d}k .$$

This equation then represents the Patterson function for a cylindrically symmetric system confined to the $k_z=0$ plane. Further, by normalizing so that $P(O)=1$:*

$$P(r) = \frac{\int_0^{\infty} I(k)J_0(kr)k\mathrm{d}k}{\int_0^{\infty} I(k)k\mathrm{d}k} . \qquad (10)$$

Thus, the Patterson function can be obtained without assumptions about the scattering system or its coherent size. However, it is not experimentally possible to reach either of the limits of integration in equation (10); nor is it possible to easily interpret $P(r)$ when full resolution is used ($k \to \infty$ in upper limit of integration).

In actual applications, the intensity data has a lower and an upper limit. The lower limit, k_1, is brought about by experimental inaccessibility near the main X-ray beam. The upper limit, k_2, is variable and, when properly chosen, allows a mathematical description of the Patterson function. For an arbitrary k_2:

$$P(r,k_1,k_2) = \frac{\int_{k_1}^{k_2} I(k)J_0(kr)k\mathrm{d}k}{\int_{k_1}^{k_2} I(k)k\mathrm{d}k} . \qquad (11)$$

Resolution in the Patterson function is a measure of the smallest details that can be resolved and is a function of k_2. The Bragg equivalent of k_2 is $d_2=2\pi/k_2$, and the maximum resolution obtained for a given k_2 is 0·6d_2. For the purpose of this series of papers, a low-resolution Patterson function is defined by $k_2 \simeq k_0$.† At this resolution the intensity can be expressed by equation (7).

---

* Henceforth, all Patterson functions are normalized.

† k_0 for a given system is a fixed point on the equator, whereas k_2 is the upper limit of the intensity data used; hence, k_2 is a free parameter. $k_2=k_0$ only for the low-resolution Patterson function.

Hence:

$$P(r,k_1,k_2)=\frac{\int_{k_1}^{k_2}\left[\frac{J_1(kR_e)}{kR_e}\right]^2\sum_{i=0}^{\bar{m}}\langle A_i\rangle J_0(kS_i)J_0(kr)\int W_i(S)J_0(kS)S\mathrm{d}S k\mathrm{d}k}{\int_{k_1}^{k_2}\left[\frac{J_1(kR_e)}{kR_e}\right]^2\sum_{i=0}^{\bar{m}}\langle A_i\rangle J_0(kS_i)\int W_i(S)J_0(kS)S\mathrm{d}S k\mathrm{d}k}. \quad (12)$$

Note that this expression for the low-resolution Patterson function is not based on a solid-cylinder model, but that the transform of the equivalent solid cylinder describes the unknown Fourier transform of the fibril very accurately at this low resolution.

The expression for the low-resolution Patterson function, equation (12), contains the parameters describing the scattering system. The left side of this equation can be calculated using intensity data from k_1 to $k_2(=k_0)$ in equation (11), thus obtaining $P(r,k_1,k_2)$. If the right side of equation (12) can be obtained as a closed-form function involving the parameters of the scattering system, then this function can be used to directly extract the parameters of the scattering system; and the problem, in principle, can be solved directly from the low-resolution Patterson function. The remainder of the paper is devoted to obtaining this closed-form function.

5. Patterson function with complete and limited resolution for a single solid cylinder

As a first step in evaluating the integrals in equation (12), the Patterson function of a single solid cylinder with complete resolution ($k_1=0$, $k_2=\infty$) is studied and then the effects of limited resolution ($k_1>0, k_2<\infty$) are evaluated.

Starting with the electron density of a solid cylinder of radius R_e:

$$\varrho(r)=\begin{cases}1 & 0\le r\le R_e,\\ 0 & r>R_e,\end{cases}$$

the normalized intensity (Oster & Riley, 1952) is

$$I(k)=\frac{4J_1^2(kR_e)}{(kR_e)^2} \quad (13)$$

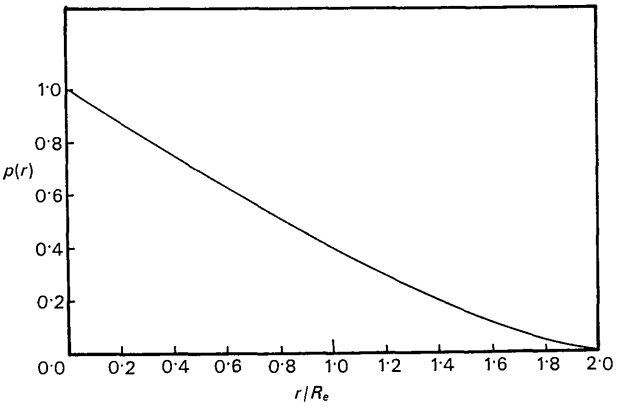

Fig. 2. Patterson function with complete resolution for a solid cylinder of radius R_e.

such that $I(O)=1$ and where $J_1(x)$ is a Bessel function of the first order.

Let $p(r)$ be the Patterson function of a single solid cylinder; thus, for a solid cylinder with complete resolution:

$$p(r)=\frac{\int_0^{\infty}\frac{J_1^2(kR_e)J_0(kr)}{k}\mathrm{d}k}{\int_0^{\infty}\frac{J_1^2(kR_e)}{k}\mathrm{d}k}=2\int_0^{\infty}\frac{J_1(kR_e)J_1(kR_e)J_0(kr)\mathrm{d}k}{k}. \quad (14)$$

Evaluation of this integral is straightforward (Harget, 1969), and the exact result is

$$p(r)=\begin{cases}\left[1-\frac{1}{\pi}\frac{r}{R_e}\sqrt{1-r^2/4R_e^2}\right.\\ \quad\left.-\frac{1}{\pi}\cos^{-1}(1-r^2/2R_e^2)\right] & 0\le r\le 2R_e\\ 0 & r\ge 2R_e\\ 1 & r=0.\end{cases} \quad (15)$$

This complete Patterson is shown in Fig. 2 as a function of r/R_e.

To study the effects of truncation, $p(r,k_1,k_2)$ must be evaluated; however, it is easier to evaluate the effects of k_1 and k_2 separately.

Let

$$p(r,k_2)=\frac{\int_0^{k_2}\frac{J_1^2(kR_e)}{k}J_0(kr)\mathrm{d}k}{\int_0^{k_2}\frac{J_1^2(kR_e)}{k}\mathrm{d}k}. \quad (16)$$

For $k_2\le k_0\le\pi/R_e$ and $O<r<R_e$, it is found (Harget, 1969) that

$$p(r,k_2)\simeq\exp\left[-\frac{\alpha^2k_2^2r^2}{4}\right]\times\left\{\frac{R_e^2}{R_e^2+r^2}\frac{\sinh\left[\frac{\alpha^2k_2^2}{4}(R_e^2+r^2)\right]}{\sinh\left[\frac{\alpha^2k_2^2R_e^2}{4}\right]}\right\}. \quad (17)$$

For all r:

$$p(r,k_2)\simeq\frac{\exp\left[-r^2/2\alpha^2R_e^2\right]}{1-\exp\left[-\frac{\alpha^2R_e^2k_2^2}{2}\right]}-\frac{\exp\left[-\frac{\alpha^2R_e^2k_2^2}{2}\right]}{1-\exp\left[-\frac{\alpha^2R_e^2k_2^2}{2}\right]}$$

$$\times \sum_{m=0}^{\infty} (-1)^m \left[\frac{k_2 r}{\alpha^2 R_e^2 k_2^2}\right]^m J_m(k_2 r) \qquad (18)$$

or

$$p(r,k_2) \simeq \frac{\exp\left[-\frac{\alpha^2 R_e^2 k_2^2}{2}\right]}{1-\exp\left[-\frac{\alpha^2 R_e^2 k_2^2}{2}\right]} \times \sum_{m=1}^{\infty} \left(\frac{\alpha^2 R_e^2 k_2^2}{k_2 r}\right)^m J_m(k_2 r)\,, \qquad (19)$$

where $\alpha^2 = \frac{9}{10}$. The accuracy and rapid convergence properties of these expressions are demonstrated in Fig. 3. Only two terms of equation (18) are required for good agreement in the range $O < r < 2R_e$ and only three terms of equation (19) are necessary for a 1–2% error in the region $2R_e < r < \infty$.

To demonstrate the behavior of $p(r,k_2)$, consider the first two terms of equation (18):

$$p(r,k_2) \simeq \frac{\exp\left[-r^2/2\alpha^2 R_e^2\right]}{1-\exp\left[-\frac{\alpha^2 R_e^2 k_2^2}{2}\right]} - \frac{\exp\left[-\frac{\alpha^2 R_e^2 k_2^2}{2}\right]}{1-\exp\left[-\frac{\alpha^2 R_e^2 k_2^2}{2}\right]} J_0(k_2 r)\,. \qquad (20)$$

From equations (17) and (20), $p(r,k_2)$ is approximately Gaussian in shape for $O < r < 2R_e$, and the broadening due to truncation can now be estimated. For $k_2 \simeq \pi/R_e$, which is the high-angle truncation value used in a low-resolution Patterson,

$$[p(R_e, \pi/R_e) - p(R_e)] \times 1{\cdot}7 R_e \simeq \delta\,,$$

where δ is the lateral increase in $p(R_e)$ due to k_2. Using equations (15) and (17):

$$\delta \simeq 0{\cdot}17\, R_e$$

or about 17% of R_e, which is not too severe.

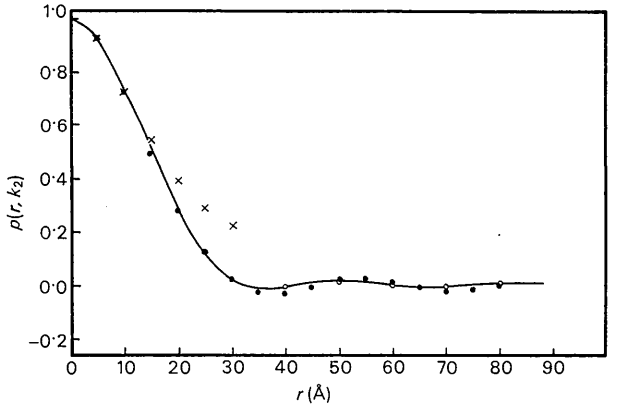

Fig. 3. Approximations for the Patterson function of a solid cylinder of radius 15 Å, $k_2 = 0{\cdot}187$ Å^{-1}. —— computer calculation of equation (16). ×——× equation (17), ●——● equation (18), (2 terms), ○——○ equation (19) (3 terms).

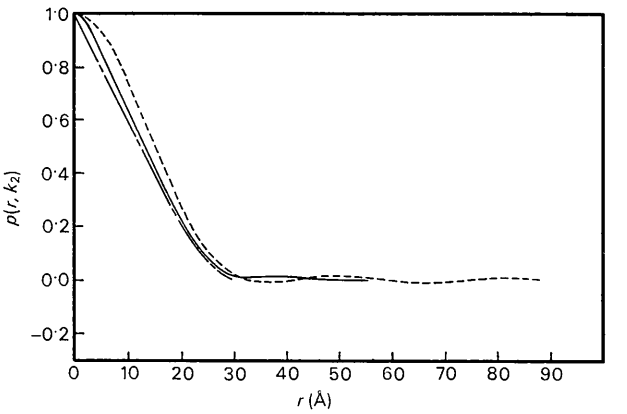

Fig. 4. High-angle truncation effects on a Patterson function for a single solid cylinder of radius 15 Å. ——— $k_2 = \infty$, – – – – $k_2 = 0{\cdot}187$ Å^{-1}, —— $k_2 = 0{\cdot}568$ Å^{-1}.

For an evaluation of the spurious fluctuations associated with high-angle truncation, consider equations (18), (19), and (20). Only the second term in equation (18) or (20) fluctuates or oscillates; thus, the first term can be ignored. The spurious oscillations have a period of approximately $d_2 = 2\pi/k_2$ because of the Bessel functions. Peak-to-peak height of the oscillations for $k_2 \simeq \pi/R_e$ is less than 0·03 or 3% since $p(O) = 1$, and this height decays as $1/r^{3/2}$ according to equation (19).

All of these high-angle truncation effects are demonstrated in Fig. 4, which is a plot of an exact $p(r,k_2)$ obtained from equation (16) *via* a computer calculation for $R_e = 15$ Å, $k_2 = 0{\cdot}187$ Å^{-1}, 0·568 Å^{-1}, and ∞.

For low-angle truncation effects let

$$p(r,k_1) = \frac{\int_{k_1}^{\infty} \frac{J_1^2(kR_e)}{k} J_0(kr)\,dk}{\int_{k_1}^{\infty} \frac{J_1^2(kR_e)}{k}\,dk}\,. \qquad (21)$$

From Harget (1969):

$$p(r,k_1) \simeq p(r) + \frac{k_1^2 R_e^2}{4}\left[p(r) - \frac{2J_1(k_1 r)}{k_1 r}\right]. \qquad (22)$$

Now k_1 is of the order of 0·02 Å^{-1} or less for actual experiments; therefore, $2J_1(k_1 r)/k_1 r \simeq 1$ for $O < r < 300$ Å.

Hence,

$$p(r,k_1) \simeq p(r) + 10^{-4} \times R_e^2[p(r) - 1]\,.$$

Thus, the correction is very small and negative. Its effects are only significant for $r > R_e$, since $p(r)$ starts at a value of 1, and merely subtracts a small constant for $2R_e < r < 300$ Å.

Combining the effects of k_1 and k_2:

$$p(r,k_1,k_2) = \frac{\int_{k_1}^{k_2} \frac{J_1^2(kR_e)}{k} J_0(kr)\,dk}{\int_{k_1}^{k_2} \frac{J_1^2(kR_e)}{k}\,dk} \qquad (23)$$

it is easily seen that

$$p(r,k_1,k_2)\simeq p(r,k_2) + 2\left\{1-\exp\left[-\frac{\alpha^2k_1^2R_e^2}{2}\right]\right\}\left[p(r,k_2)-\frac{2J_1(k_1r)}{k_1r}\right]. \quad (24)$$

Exact computer calculations of equations (23) and (16) are shown in Fig. 5, which demonstrates the effects of low-angle truncation.

In conclusion, the truncation effects of k_1 and k_2 developed in this section cause only small perturbations of $p(r)$. Consequently, when studying the truncated Patterson of many solid cylinders, these perturbations can be recognized and evaluated.

6. Patterson function with complete resolution for a group of solid cylinders

The next step in evaluating equation (12) is to study this Patterson function when there is complete resolution ($k_1=0$, $k_2=\infty$). For simplicity, average values of the A_i's are ignored, and for clarity, distortion effects are neglected here. Equation (12) then becomes:

$$P(r)=\frac{\sum_{i=0}^{m}A_i\int_0^\infty \frac{J_1^2(kR_e)J_0(kS_i)J_0(kr)\mathrm{d}k}{k}}{\sum_{i=0}^{m}A_i\int_0^\infty \frac{J_1^2(kR_e)J_0(kS_i)\mathrm{d}k}{k}}. \quad (25)$$

Now

$$S_0=0 \quad \text{and} \quad 2\int_0^\infty \frac{J_1^2(kR_e)J_0(kr)\mathrm{d}k}{k}=p(r).$$

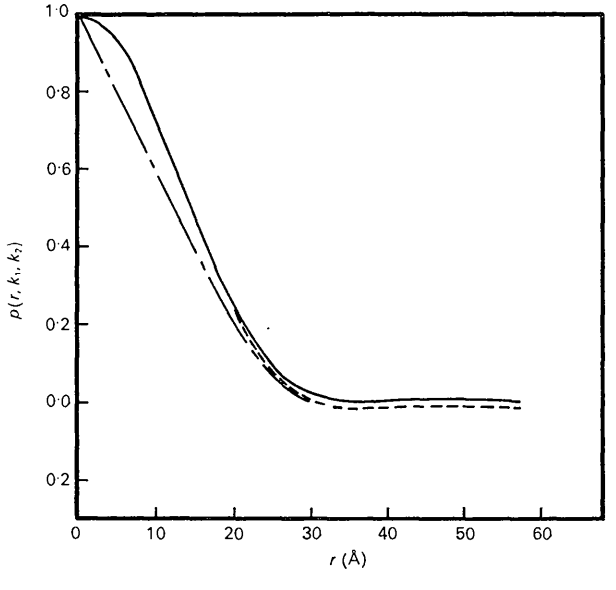

Fig. 5. High- and low-angle truncation effects on a Patterson function for a single solid cylinder of radius 15 Å. —— – —— $p(r)$, ——$p(r,0,0{\cdot}259)$, – – – –$p(r,\ 0{\cdot}019,\ 0{\cdot}259)$.

Also,

$$p(x>2R_e)=0 \quad \text{and} \quad S_i>2R_e \text{ for } i=1,2,\ldots m.$$

Thus,

$$\int_0^\infty \frac{J_1^2(kR_e)J_0(kS_i)\mathrm{d}k}{k}=0 \quad \text{for} \quad i>0.$$

Also, let

$$\int_0^\infty \frac{J_1^2(kR_e)J_0(kS_i)J_0(kr)\mathrm{d}k}{k}=g_i(r). \quad (26)$$

Then equation (25) reduces to

$$P(r)=p(r)+\frac{2}{A_0}\sum_{i=1}^{m}A_ig_i(r). \quad (27)$$

In this form it is seen that the Patterson function of a single solid cylinder is located at the origin of $P(r)$, as expected, and that it can be evaluated to obtain R_e. Also, as shown by Harget (1969), $g_i(r)=0$ except in the region

$$S_i-2R_e\le r\le S_i+2R_e. \quad (28)$$

Thus, a peak is also located at each S_i in $P(r)$.

Now $g_i(r)$ is not an easy integral to evaluate. It is a complicated expression involving elliptic integrals of the second kind, but it suffices to say that $g_i(r)$ is approximately symmetric about S_i and has a shape similar to $p(r)$. Also, the maximum value of $g_i(r)$ is $g_i(S_i)$, and it can be shown (Harget, 1969) that

$$g_i(S_i)=\frac{R_e}{2\pi S_i}\int_0^2 \frac{p(x)\mathrm{d}x}{\sqrt{1-\frac{R_e^2x^2}{4S_i^2}}}$$

or

$$g_i(S_i)\simeq\frac{R_e}{2\pi S_i}\left\{\frac{8}{3\pi}+\frac{32}{45\pi}\left(\frac{R_e}{2S_i}\right)^2+\ldots\right\}, \quad (29)$$

Thus, the S_i's can be obtained from $P(r)$ simply by observing the positions of the peaks in the Patterson function. In addition, A_i/A_0 can be obtained for the ith peak by measuring the peak height and using:

$$\text{peak height}=2g_i(S_i)A_i/A_0. \quad (30)$$

Note that A_i/A_0 is simply the ith nearest-neighbor number for the ith peak. These nearest-neighbor numbers are characteristic of the geometry and coherent size of the scattering system and have the same meaning as those used in a radial distribution function.

In addition, if the coherent size of the scattering system is very large it can be shown (Harget, 1969) that

$$P(r)=\Omega=\frac{N}{V}\pi R_e^2 \quad (\text{for large } r), \quad (31)$$

and hence the volume fraction occupied by the fibrils can be obtained.

Thus, in principle, all physical parameters describing the scattering system can be obtained once the

Patterson function, with complete resolution, is calculated. Unfortunately, complete resolution cannot be obtained simply because a low-angle truncation, k_1, is imposed by experimental equipment and a high-angle truncation, k_2, is purposely imposed so that equation (25) is valid. However, if the effects of k_1 and k_2 on $P(r)$ of equation (27) can be evaluated, then in principle the physical parameters can again be obtained.

7. Patterson function with limited resolution for a group of solid cylinders

The final step in evaluating equation (12) is to study the effects of low-angle and high-angle truncation on the Patterson function with complete resolution. For simplicity average values of the A_i's are again ignored, along with distortions, and for clarity the effects of k_1 and k_2 are evaluated separately and then combined.

For high-angle truncation (recalling that the upper limit is purposely imposed so that equation (25) is valid),

$$P(r,k_2)=\frac{\sum_{i=0}^{m} A_i \int_0^{k_2} \frac{J_1^2(kR_e)}{k} J_0(kS_i)J_0(kr)\mathrm{d}k}{\sum_{i=0}^{m} A_i \int_0^{k_2} \frac{J_1^2(kR_e)}{k} J_0(kS_i)\mathrm{d}k}. \qquad (32)$$

This can be expressed (Harget, 1969) as:

$$P(r,k_2)\simeq p(r,k_2) + \left\{\frac{9}{8}\frac{1}{1-\exp\left[-\frac{9}{32}R_e^2k_2^2\right]}\right\}\frac{2}{A_0}\sum_{i=1}^{m} A_i g_i(r,k_2). \qquad (33)$$

This is in a form very similar to $P(r)$ of equation (27). Also, $p(r,k_2)$ was fully discussed in § 5, and the only new function is $g_i(r,k_2)$. This function could be evaluated for all r (Harget, 1969), but it is a very complicated expression and is similar to $g_i(r)$; therefore, it is only of interest in the region $S_i-2R_e<r<S_i+2R_e$. In this region:

$$g_i(r,k_2)\simeq\tfrac{4}{9}\left\{\exp\left[-\frac{8}{9R_e^2}(S_i-r)^2\right]\exp\left[-\frac{16S_ir}{9R_e^2}\right] \times I_0\left(\frac{16S_ir}{9R_e^2}\right)-\exp\left[-\frac{9R_e^2k_2^2}{32}\right] \times J_0(k_2S_i)J_0(k_2r)\right\}, \qquad (34)$$

where I_0 is a modified Bessel function (Bessel function with an imaginary argument).

To demonstrate the accuracy of these equations, consider Fig. 6 where an exact Patterson function obtained by computer calculation of equation (32) for a model system is shown, along with the approximations of equations (33) and (34) in the regions $S_i-2R_e<r<S_i+2R_e$. It is concluded that at S_i, equations (33) and (34) are accurate to within 1 or 2%.

Although equation (34) appears to be complex, several of its features can be readily established. The first term in this expression is the dominant one, and the second is merely a small correction. In addition, $\exp(-x)I_0(x)$, which is tabulated in tables of Bessel functions, is slowly varying compared to the Gaussian distribution about S_i; therefore, the ith peak is approximately Gaussian in shape. Its maximum is at $r=S_i$* and its half-width, HW_i, according to the half-width of a Gaussian curve, is

$$HW_i\simeq 1{\cdot}8\ R_e. \qquad (35)$$

Finally, the most important feature of this expression, the peak height at $r=S_i$, is obtained by using equations (33) and (34):

$$\text{Peak height}\simeq\frac{A_i}{A_0}\frac{1}{1-\exp\left[-\frac{9}{32}R_e^2k_2^2\right]} \times\left\{\exp\left[-\frac{16S_i^2}{9R_e^2}\right]I_0\left(\frac{16S_i^2}{9R_e^2}\right) -\exp\left[-\tfrac{9}{32}R_e^2k_2^2\right]J_0^2(k_2S_i)\right\}. \qquad (36)$$

To calculate the effects of low-angle truncation, an expression of the form:

$$P(r,k_1)=\frac{\sum_{i=0}^{m} A_i \int_{k_1}^{\infty} \frac{J_1^2(kR_e)}{k} J_0(kS_i)J_0(kr)\mathrm{d}k}{\sum_{i=0}^{m} A_i \int_{k_1}^{\infty} \frac{J_1^2(kR_e)}{k} J_0(kS_i)\mathrm{d}k} \qquad (37)$$

must be evaluated. Recalling that k_1 is experimentally imposed by how close observations can be made to the main beam, two important cases for evaluating this expression have been worked out (Harget, 1969).

Case (1): when the scattering system has limited coherence such that the 000 reflection extends far enough to be intersected by k_1, then:

$$P(r,k_1)\simeq\frac{P(r)-\frac{R_e^2N}{\chi^2}q(r,\chi,k_1)}{1-\frac{R_e^2N}{\chi^2}\left\{1-\exp\left[-\frac{\chi^2k_1^2}{4}\right]\right\}}, \qquad (38)$$

where

$$q(r,\chi,k_1)=\exp[-r^2/\chi^2]-\exp\left[-\frac{\chi^2k_1^2}{4}\right] \times\sum_{n=0}^{\infty}(-1)^n\left(\frac{2k_1r}{\chi^2k_1^2}\right)^n J_n(k_1r) \qquad (39a)$$

or

$$q(r,\chi,k_1)=\exp\left[-\frac{\chi^2k_1^2}{4}\right]\sum_{n=1}^{\infty}\left(\frac{\chi^2k_1^2}{2k_1r}\right)^n J_n(k_1r), \qquad (39b)$$

* $\exp(-x)I_0(x)$ is a monotonically decreasing function and may cause a very small shift of the $i=1$ peak toward the origin of Patterson space.

where:

$$\chi^2 = \sum_{i=1}^{m} A_i S_i^2 / N^2, \tag{40}$$

and N = total number of particles scattering coherently.

Thus, no really new information is added by these parameters since they are a combination of the A_i's and S_i's.

The effect of this low-angle truncation of the Patterson function is seen quite easily from equations (38) and (39). The only varying contribution (function of r) is $q(r,\chi,k_1)$, but this function is identical in form to the function $p(r,k_2)$ which has been studied previously. It is approximately Gaussian in shape out to 2χ, where it becomes small and starts to oscillate. Thus, the Patterson function can now have negative values. Also, the period of $q(r,\chi,k_1)$ is much greater than that of $p(r)$ or $g_i(r)$; consequently, $q(r,\chi,k_1)$ can be separated easily from the rest of the Patterson function. In fact, the effect of low-angle truncation can be considered as merely a modulation of $P(r)$ with the slowly varying function $q(r,\chi,k_1)$.

Case (2): when the scattering system is infinite in extent (in the micron range), such that the 000 reflection is a delta function located at the origin, then:

$$P(r,k_1) \simeq \frac{P(r)-\Omega}{1-\Omega}, \tag{41}$$

where $\Omega = \pi R_e^2 \varrho_0$ and ϱ_0 = density of scattering centers. This is an extremely simple effect because Ω is a constant.

The combined effect of low- and high-angle truncation is now very easy to formulate:

$$P(r,k_1,k_2) = \frac{\int_0^{k_2} I(k)J_0(kr)k\mathrm{d}k - \int_0^{k_1} I(k)J_0(kr)k\mathrm{d}k}{\int_0^{k_2} I(k)k\mathrm{d}k - \int_0^{k_1} I(k)k\mathrm{d}k}.$$

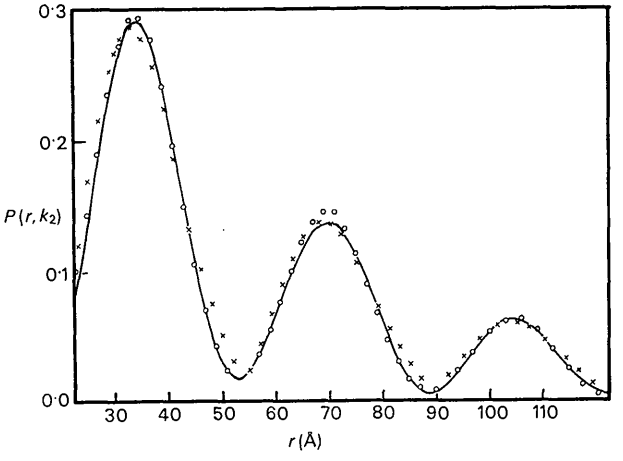

Fig. 6. Approximations for the many-particle Patterson function, $P(r,k_2)$. $R = 10$ Å, $k_2 = 0{\cdot}2728$ Å^{-1}. ——$P(r,k_2)$ from equation (32). For the region $S_i - 2R < r < S_i + 2R$. ○——○ from equations (33) and 1st term of (34). ×——× from equations (33) and (34).

Dividing both numerator and denominator by

$$\int_0^{k_2} I(k)k\mathrm{d}k$$

this becomes:

$$P(r,k_1,k_2) = \frac{P(r,k_2) - \dfrac{\int_0^{k_1} I(k)J_0(kr)k\mathrm{d}k}{\int_0^{k_2} I(k)k\mathrm{d}k}}{1 - \dfrac{\int_0^{k_1} I(k)k\mathrm{d}k}{\int_0^{k_2} I(k)k\mathrm{d}k}}. \tag{42}$$

For case (1),

$$\int_0^{k_1} I(k)k\mathrm{d}k \simeq \frac{2}{\chi^2}\left[1 - \exp\left[-\frac{\chi^2 k_1^2}{4}\right]\right]$$

$$\int_0^{k_1} I(k)J_0(kr)k\mathrm{d}k \simeq \frac{2}{\chi^2} q(r,\chi,k_1).$$

For the last integral, recalling that $I(O)$ must be normalized to 1:

$$\int_0^{k_2} I(k)k\mathrm{d}k = \frac{1}{N^2}\sum_{i=0}^{m} A_i \int_0^{k_2} \frac{4J_1^2(kR_e)}{(kR_e)^2} J_0(kS_i)k\mathrm{d}k$$

$$\int_0^{k_2} I(k)k\mathrm{d}k = \frac{1}{N}\int_0^{k_2} \frac{4J_1^2(kR_e)}{(kR_e)^2} k\mathrm{d}k + \sum_{i=1}^{m} \frac{A_i}{N^2} p(S_i,k_2).$$

But only the $i=0$ term is significant and

$$\int_0^{k_2} \frac{4J_1^2(kR_e)}{(kR_e)^2} k\mathrm{d}k \simeq \frac{16}{9R_e^2}\{1 - \exp[-\tfrac{9}{32}R_e^2 k_2^2]\}.$$

Thus,

$$\int_0^{k_2} I(k)k\mathrm{d}k \simeq \frac{16}{9R_e^2}\frac{1}{N}\{1 - \exp[-\tfrac{9}{32}R_e^2 k_2^2]\}.$$

By inserting these integrals in equation (42), the final result is:

$$P(r,k_1,k_2) \simeq \frac{P(r,k_2) - \left\{\frac{9}{8}\dfrac{1}{1-\exp[-\frac{9}{32}R_e^2k_2^2]}\right\}\dfrac{NR_e^2}{\chi^2} q(r,\chi,k_1)}{1 - \left\{\frac{9}{8}\dfrac{1}{1-\exp[-\frac{9}{32}R_e^2k_2^2]}\right\}\dfrac{NR_e^2}{\chi^2}\left\{1 - \exp\left[-\dfrac{\chi^2k_1^2}{4}\right]\right\}}. \tag{43}$$

This final expression is no more complex than equation (38) for $P(r,k_1)$, except that there is now a constant, $\frac{9}{8}\dfrac{1}{1-\exp[-\frac{9}{32}R_e^2k_2^2]}$, and $P(r,k_2)$ is substituted for $P(r)$.

For case (2), proceeding in a similar fashion:

$$P(r,k_1,k_2) \simeq \frac{P(r,k_2) - \left\{\frac{9}{8}\dfrac{1}{1-\exp[-\frac{9}{32}R_e^2k_2^2]}\right\}\Omega}{1 - \left\{\frac{9}{8}\dfrac{1}{1-\exp[-\frac{9}{32}R_e^2k_2^2]}\right\}\Omega}, \tag{44}$$

which is analogous to equation (41).

This then completes the development of $P(r,k_1,k_2)$, and the integrals in equation (12) have been reduced to functions of the parameters which describe the scattering system.

8. Summary

Mathematical expressions for the equatorial intensity have been presented which involve the Fourier transform of the fibril, interfibrillar interference function, and effects of lattice distortions in a quantitative manner. Also, allowances have been made for the effects of structural inhomogeneities by leaving the coherent size as a free parameter and allowing for the possibility of an additional scattering component due to associated electron-density fluctuations. One of the most important features of these equations is that the functional form of the Fourier transform of the fibril is known in the region $0<k<k_0$ and involves only a single parameter, R_e, which can be related to the radius of gyration of the fibril. It is emphasized that this expression for the fibril is not a model but a modification of the Guinier approximation and holds very well for $k<k_0$.

Mathematical expressions for the low-resolution Patterson function have also been derived, and their accuracy has been demonstrated to be within a few percent. Techniques for the use of these expressions, along with a different approach, are presented in the next paper of this series, where lattice distortions and higher-resolution data are also considered.

This research was supported by U.S. Public Health Service Grant AM02830.

References

ASTBURY, W. T. (1949. *Exp. Cell. Res.* Suppl. 1, 234.
ASTBURY, W. T. & SPARKS, L. C. (1947). *Biochim. Biophys. Acta,* **21**, 177.
ASTBURY, W.T. & WEIBULL, C. (1949). *Nature, Lond.* **163**, 280.
BEAR, R. S. & BOLDUAN, O. E. A. (1950). *Acta Cryst.* **3**, 230.
BURGE, R. E. (1961). *Proc. Roy. Soc.* A **260**, 558.
BURGE, R. E. (1963). *J. Mol. Biol.* **7**, 213.
COREY, R. B. & WYCKOFF, R. W. G. (1936). *J. Biol. Chem.* **114**, 407.
ENGSTROM, A. & FINEAN, J. B. (1953). *Nature, Lond.* **171**, 564.
GUINIER, A. & FOURNET, G. (1955). *Small Angle Scattering of X-rays,* p. 27. New York: John Wiley.
HARGET, P. J. (1969). Ph.D. Thesis, Univ. of Michigan.
HEIKENS, D., HERMANS, P. H. & WEIDINGER, A. (1952). *Nature, Lond.* **170**, 369.
HEYN, A. N. J. (1948). *J. Amer. Chem. Soc.* **70**, 3138.
HEYN, A. N. J. (1955). *J. Appl. Phys.* **26**, 1113.
HOSEMANN, R. (1951). *Acta Cryst.* **4**, 520.
HOSEMANN, R. (1967). *In Small-Angle X-ray Scattering.* Ed. by H. BRUMBERGER. New York: Gordon and Breach.
HOSEMANN, R. & BAGCHI, S. N. (1962). *Direct Analysis of Diffraction by Matter,* Chapter XII. Amsterdam: North-Holland.
JAMES, R. W. (1948). *Optical Principles of X-ray Diffraction,* pp. 503, 584, 400. London: Bell.
KRIMM, S. (1963). *Acta Cryst.* **16**, A82.
KRIMM, S. (1967). In *Small-Angle X-ray Scattering.* Ed. by H. BRUMBERGER. New York: Gordon and Breach.
NORTH, A. C. T., COWAN, P. M. & RANDALL, J. T. (1954). *Nature, Lond.* **174**, 1142.
OSTER, G. & RILEY, D. P. (1952). *Acta Cryst.* **5**, 272.
SASISEKHARAN, V. & RAMACHANDRAN, G. N. (1957). *Proc. Indian Acad. Sci.* **45**, 363.

Acta Cryst. (1971). A **27**, 596

Direct Evaluation of $K\alpha_1$ Fourier Coefficents in X-ray Profile Analysis

BY A. KIDRON AND R. J. DE ANGELIS

Department of Metallurgical Engineering and Materials Science, University of Kentucky, Lexington, Kentucky 40506, *U.S.A.*

(*Received* 19 *January* 1971)

Using a least-squares method of analyzing X-ray diffraction profiles, it is shown that one can calculate directly the Fourier coefficients of the $K\alpha_1$ component from the total $K\alpha$ doublet intensities. These Fourier coefficients can be calculated around any preferred points of the profile, *e.g.* the center of gravity or peak of the profile of $K\alpha_1$.

Introduction

Fourier analysis of X-ray diffraction lines normally requires that the intensity be given for the $K\alpha_1$ component alone. To this end a few methods of separating the $K\alpha$ doublet have been proposed. The works of Brill (1928), Jones (1938) and Finch (1949) all assume that the $K\alpha_1$ profile has a known functional form (*e.g.* Gaussian). This assumption is not valid in the case of line profiles taken from deformed materials (Warren, 1960) where Fourier analysis is extensively used. Also, the assumption of Papoulis (1955) that the profile is